Automatic Landing Method of a Reclaimer on the Stockpile

Chintae Choi, Kwanhee Lee, Kitae Shin, Keum Shik Hong, and Hyunsik Ahn

Fig. 1. Reclaimer approaching the pile.

Abstract—Large excavation reclaimers, in the raw ore yards of steel production facilities, are used to dig ore and transfer it to the blast furnaces that refine the ore into pure metal form. The reclaiming job consists of two operations: 1) landing reclaimer buckets on the surface of a pile and 2) slewing its boom with rotating buckets to scoop the ore. It is still very hard task even for very experienced workers to land the large reclaimer on the pile without collision. In this paper, an automatic landing method for choosing where to dig in a pile of raw ore is firstly proposed to achieve autonomous reclaiming. The method from this work is comprised of detecting the shape of a pile, extraction of contour lines of the pile, obtaining the joint angles of the reclaimer and determination of an optimal landing point.

A three-dimensional (3-D) range finder was developed with laser radar concepts to detect the shape and height of the ore pile. A series of image processing techniques for extracting the contour line from the 3-D range data of a pile is suggested for real implementation in this scheme. A height map is obtained from the acquired range data for a pile and a contour map for the pile is obtained through image processing steps including interpolation and edge following.

The optimal landing point of the bucket on the contour line is determined so that an overload problem does not occur in the slewing operation and reclaiming efficiency can be maximized. The algorithm for finding the landing point requires an inverse kinematics solution for the reclaimer.

The forward kinematics of the reclaimer is firstly obtained and it is verified through the kinematics of the reclaimer that the reclaimer has a redundancy due to the wheel of rotating buckets at the end of its boom. A constraint equation based on the geometrical relationship is suggested to solve the inverse kinematics of the reclaimer with redundancy. The proposed method was successfully applied to the working reclaimer. The first autonomous reclaimer in the world is being operated now in the yards of Kwangyang Steelworks in Korea.

I. INTRODUCTION

In a steel company, stock yards contain piles of raw ore for later transfer to the blast furnaces at a scheduled time. In managing the piles of raw ore, reclaimers are used to dig out the raw ore and put it on the conveyer belt for transferring it to the blast furnaces. A reclaimer is very large, about 25 m high, 50 m in length, and looks like a large crane. It has a 45-m boom and a rotating disk with buckets at the end point of the boom for scooping raw ore as shown in Fig. 1. It has three degrees of free motion; a linear translation axis on the rail, a slewing axis and a pitching axis of the boom for approaching the pile. Generally the reclaiming job is done by two-stage operations: landing the reclaimer buckets on the surface of the pile and slewing the boom with the rotating buckets while the translation and pitching axes are fixed for easy and safe reclaiming job management. After slewing from the starting point to the end point, the reclaimer translates about 30 cm for the next slewing. If we want to change the digging level, the pitching angle can be changed. Until now, landing operations have been done via remote control by very
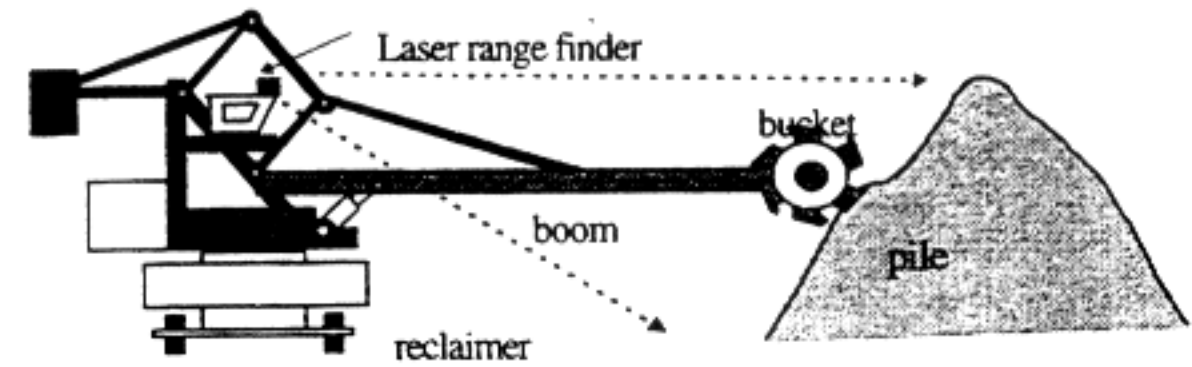
experienced workers with the aid of some video cameras attached to the reclaimer.

In the current telemanipulative approach, the worker moves the three axes of the reclaimer by handling joysticks while watching the monitor in the main control room [1], [2]. However, the operation is not easy, because the image on the monitor cannot show the exact shape of the pile at night or in especially bad weather. Other approaches use ultrasonic sensors to detect only the distance between buckets and the pile [3]. If the reclaimer collides with the pile or another machine, the reclaimer can cause serious problems. So we need to develop an automation system for the reclaimer. The most important function of the autonomous reclaimer is to detect a landing point on the surface of the pile and let the buckets land on it automatically without collision. The landing operation has been an obstacle to the full automation system for the material handling in the stock yards.

In this paper, an automatic landing method of the reclaimer is firstly proposed. To the best knowledge of the authors, no published results for automatic landing methods of reclaimer on the stockpile or other related subjects are found in the literature yet. It is assumed that overload occurs in the buckets if the buckets dig ore more deeply in the pile than the prescribed depth of the bucket in the slewing operation. If the buckets are deeply embedded in the pile, it can not dig out ore. Therefore, the operation is stopped because of severe overload.

A series of image processing techniques are integrated and applied to extract contour lines from the range data of the stockpile captured by a three-dimensional (3-D) range finder in this scheme. To detect the shape of the pile, a 3-D range finder which consists of a two-dimensional scanner and an additional joint is developed with laser radar concepts and is installed on the roof of the reclaimer [4], [5]. A height map is obtained from the acquired range data for an ore pile and a contour map for the pile is obtained through some image processing steps [6]. The contour lines in the map become landing points on which the buckets of the reclaimer can land. Possible landing points are defined as ones that do not bring about the overload in the slewing operation. An optimal landing point in the contour line is determined so that the overload problem does not occur in the slewing operation and digging efficiency is maximized, simultaneously.

The algorithm for finding the optimal landing point needs an inverse kinematics solution for the reclaimer. A solution of the inverse kinematics for the reclaimer and an algorithm for determining an optimal landing point are firstly suggested in this research.

Since the wheel of rotating buckets at the end of the boom is considered as the end-effector with one degree of freedom, the reclaimer kinematics has redundant freedom. To solve the problem of the inverse kinematics, a constraint equation was derived using the contact relationship with the surface of the pile. The automation system with a 3-D range finder and automatic landing capability was
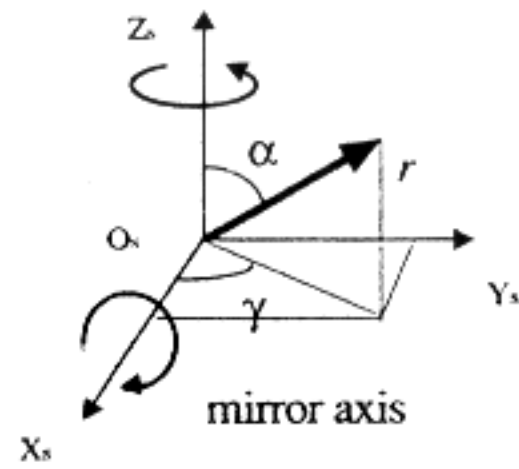
Fig. 2. Spherical coordinate system of the range finder.

fully applied to the reclaimer in the raw ore yard of the iron-making works and showed satisfactory results.

II. DESCRIPTION OF RANGE-FINDING SYSTEM INSTALLED

To obtain three 3-D shape of the pile, a laser range finder which has two scanning axes was installed with a distance from the sensor to the target pile of about 45 m. The range finder has a large field of view, more than 70° vertically and 270° horizontally. It has a long-range point sensor, a rotating mirror for vertical scanning and a swivel joint for horizontal scanning. The point sensor is a time-of-flight laser range finder providing a range accuracy of ±3 cm. The scanning speed of the sensor is 8 rot/s and the sampling rate is about 3000 Hz. When the host computer controlling the reclaimer receives a command from the supervisory computer, the reclaimer approaches the target pile and stops approximately at the proper position. Then, the range finder scans the front part of the pile which the reclaimer is paused. The height and width of the pile are, in general, about 15 and 30 m, respectively. Range data in the spherical coordinate system centered on the optical center of the range finder are acquired by encoding the step angles of the two rotating axes and detecting the depths of the points in the pile. The range data in the spherical coordinate system (r, α, γ) are transformed into the Cartesian coordinate system (x_s, y_s, z_s) as shown in Fig. 2.

$$x_s = r \sin \alpha \cos \gamma$$
$$y_s = r \sin \alpha \sin \gamma$$
$$z_s = r \cos \gamma. \tag{1}$$

The range data in the local coordinate system are transformed to the world coordinate system by geometric translation and rotation.

A height map is generated by mapping the range data in the Cartesian coordinate system with the intensity value in the (U, V) image plane Fig. 3.

The unit steps of the (U, V) axes are selected according to the resolution of 3-D profile data. Since the range data in the height map are expressed as sparsely scattered points from the optic center of the range finder, it is necessary to interpolate the range data to construct a 3-D profile map. First, the two pixels which were computed from the neighboring range data through the scanning step of a rotating mirror are linearly interpolated. Second, linear interpolation through the swivel scanning axis is added like the mirror axis interpolation as shown in Fig. 4.

In spite of interpolations, there are many missing regions in the height map due to occlusion. The missing points can be reduced with denser scanning, but it needs a great deal of memory and large execution time in the computer which are not realizable in the real implementations. The missing regions are merged linearly through the U or V axis. To merge the missing regions, the gray value of the pixels are examined along the V or U axis. The pixels which have no gray value are linearly interpolated by the gray values of the nearby pixels having gray level. Fig. 5 shows the merged image for the front part of the pile. After low pass filtering for noise reduction, the height
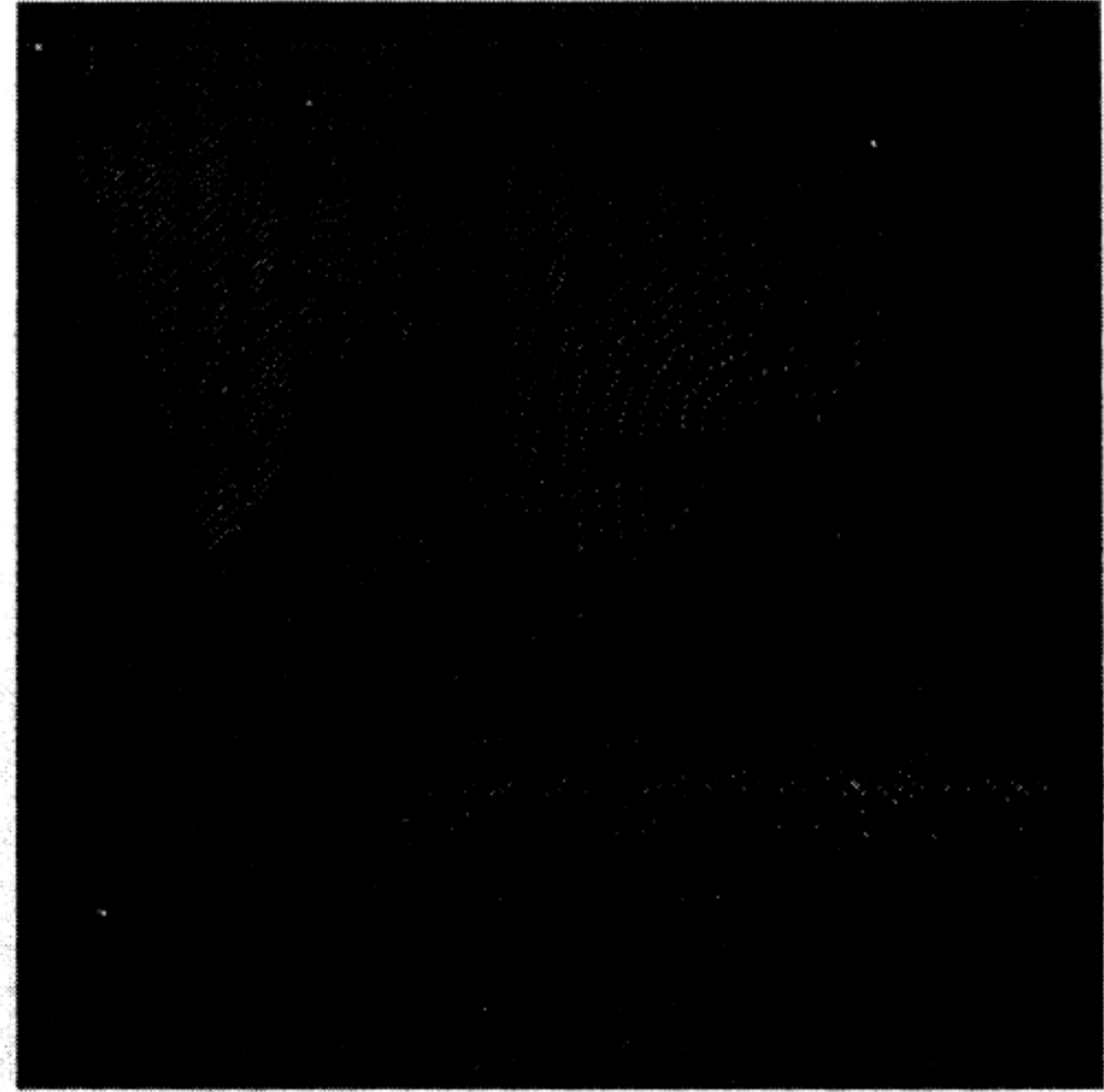

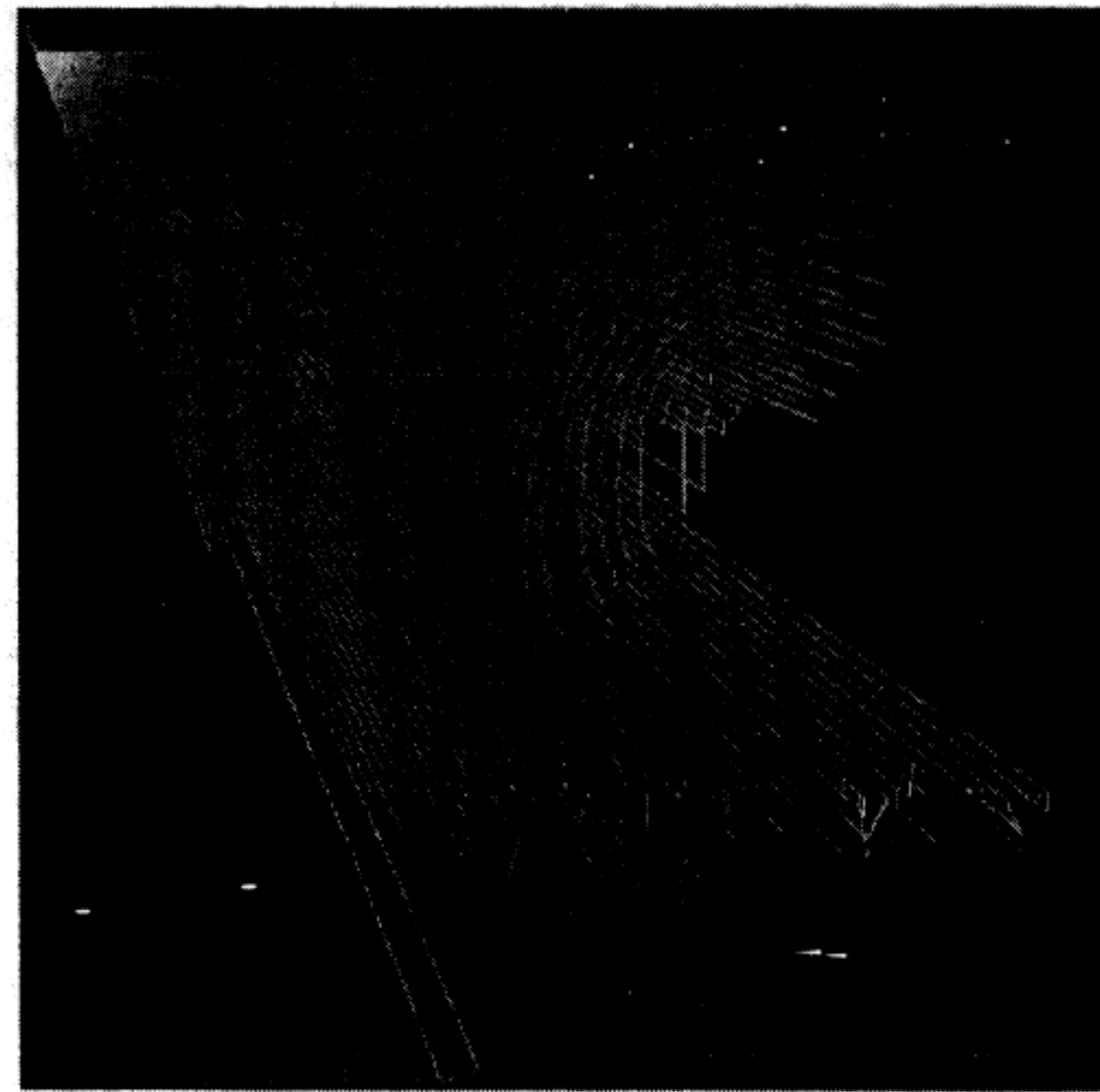Fig. 3. Topographic height map of range data array (top view).

Fig. 4. Interpolated image of the topographic height map.

map represents the 3-D profile map revealing the real X, Y, and Z coordinate of the object pile.

The merged image still has occluded regions having no gray values as shown in the figure. The regions can bring about problems that there exist more than one sliced image in the vicinity of the highest regions of the merged height map in the processing step of the contour line extraction. Therefore, the occluded regions are interpolated with gradually decreasing gray value in the radial direction and are also merged to bear the final height map for extracting contour lines. Fig. 6 shows the results of interpolation and merging of the height map.
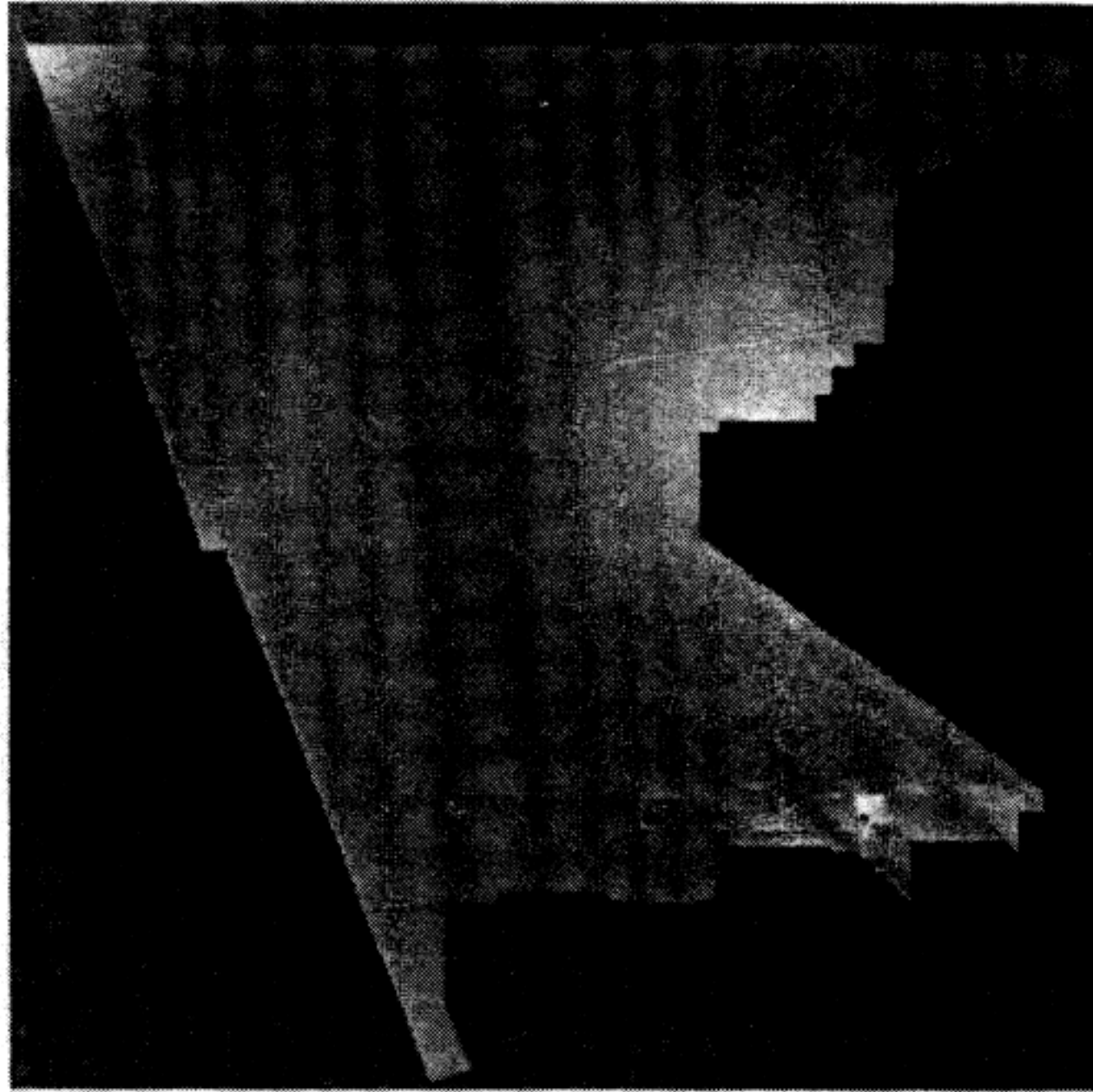
Fig. 5.　Merged image of the height map.

In the final image processing step, the contour lines for the landing height of the buckets are extracted. Sliced images corresponding to the contour lines are obtained by thresholding the height map from the prior image processing step. Since the back side of the sliced image consists of false data by image processings and has no relation with determination of the landing point, it is cut out from the image. Fig. 7 illustrates the procedure for contour line extraction.

The highest point in the height map and the center line of the horizontal scanning angle are obtained, respectively. Then, the split line which passes the highest point and perpendicularly crosses the center line is obtained. The rear region of the split line in the sliced image are excluded from consideration. A contour line is extracted from the edge points in the front side of the split line in the sliced image by using the edge following technique [7]. In the edge following technique, the border can get lost. Therefore it is slightly modified to prevent losing the border in this scheme. The candidates of the feasible borders are saved for later use and the procedure starts from the candidates when the borders get lost. Fig. 8 shows the extracted contour map that can be used to determine a landing point.

III. INVERSE KINEMATICS OF A RECLAIMER

The autonomous reclaimer is servoed in the joint-variable space, whereas the points on the pile are expressed in the world coordinate system. In order to control the position of the bucket to reach the points, the inverse kinematics solution should be solved. The disk-like end-effector has an action to produce another degree of freedom when it lands on the pile. Fig. 9 shows the assignment of link frames for the reclaimer. A Cartesian coordinate system $X_i Y_i Z_i$ can be established for each link at its joint axis with the reference coordinate system $X_0 Y_0 Z_0$. o and v are the fixed angles between the boom and the rotating disk by the mechanical structure.

v helps the reclaimed ore fall onto the conveyor belt on the boom. Let (x_d, y_d, z_d) be a point on the pile. We would like to find the corresponding joint angles, θ_2 and θ_3, and translation distance d_1 of the reclaimer so that the bucket can be positioned as desired. θ_2 and θ_3 are the slewing and pitching angles of the boom, respectively. θ_1 is an angle between z_0 and the contact point with the pile. It
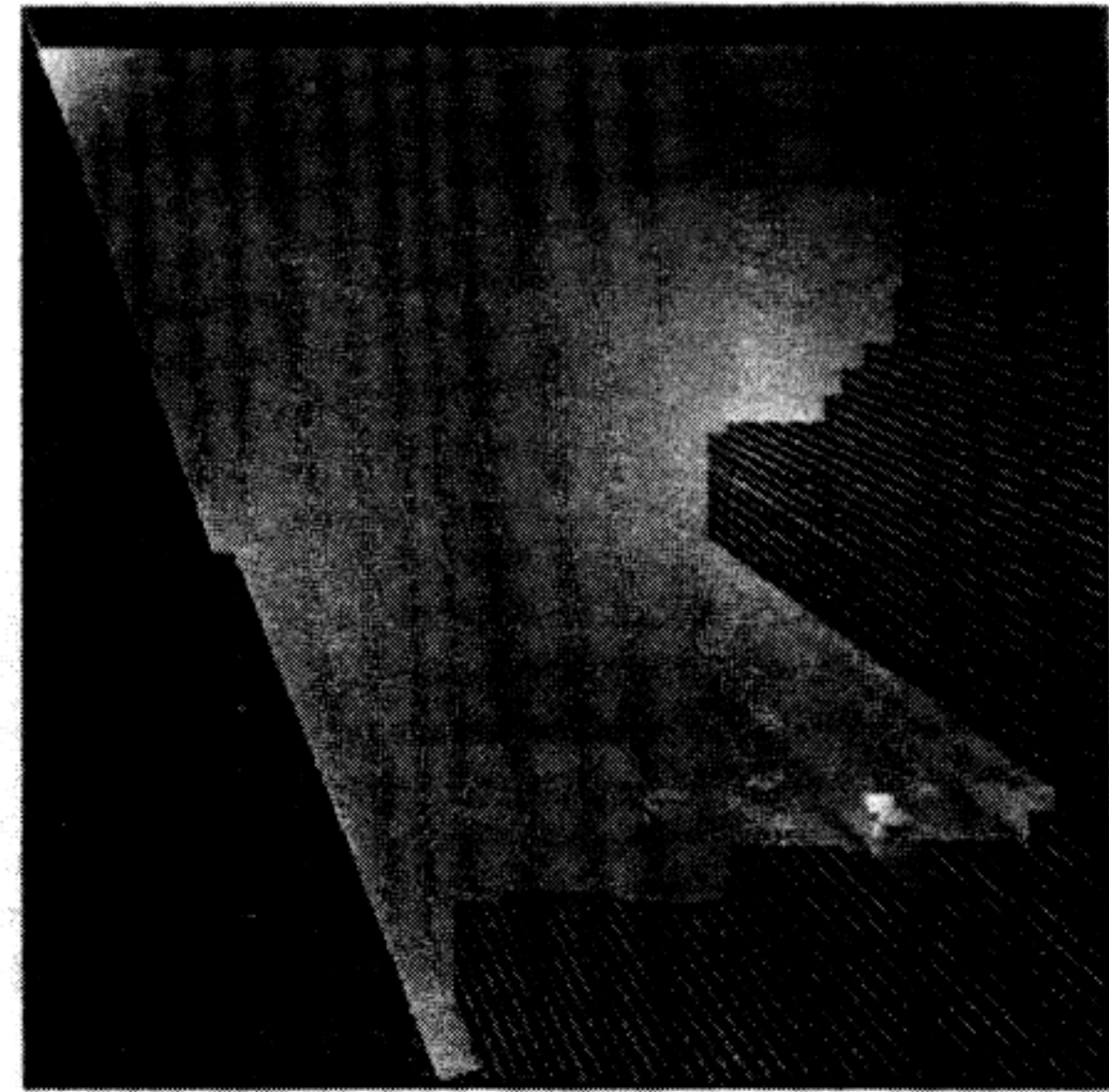
(a)
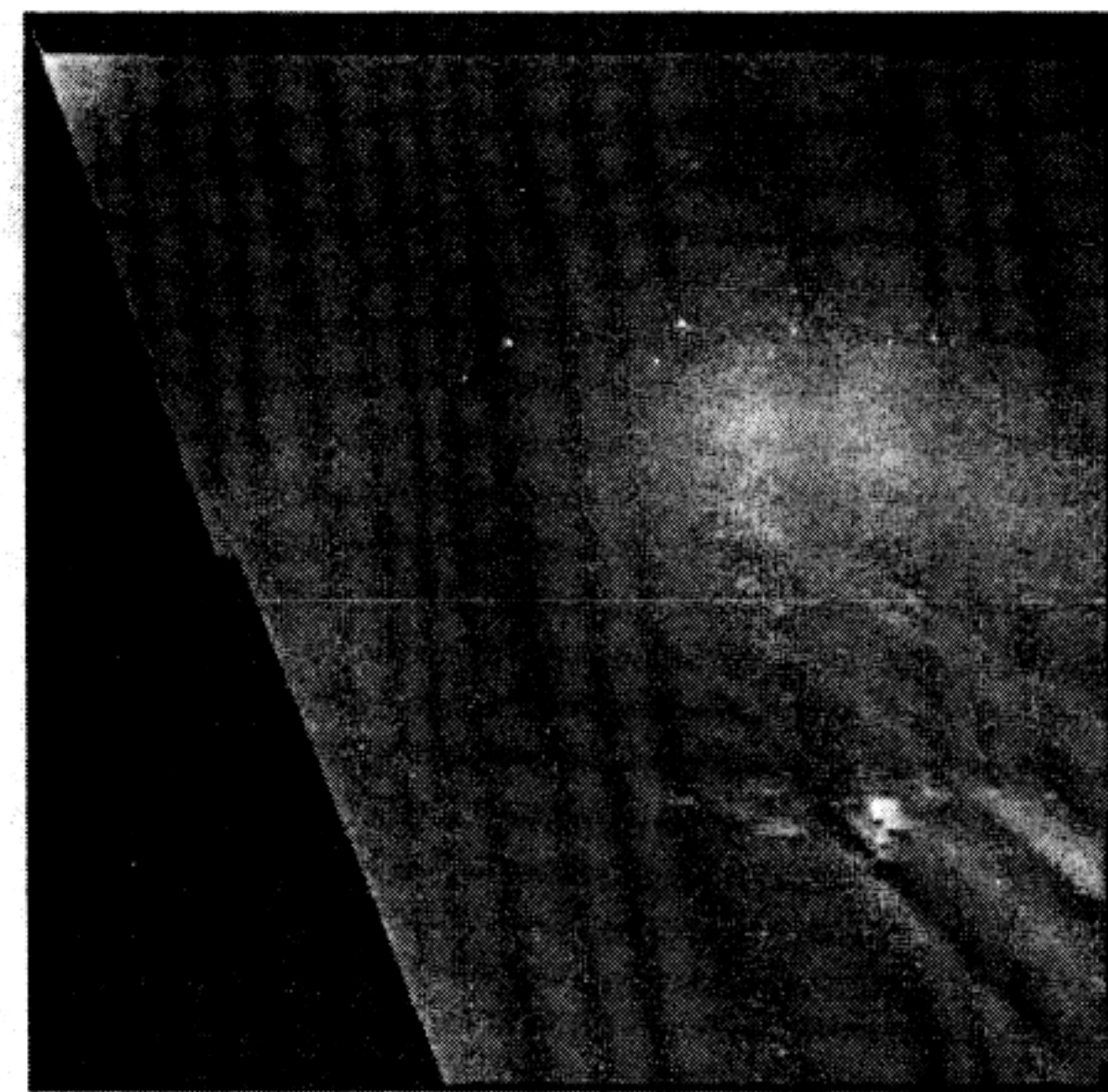
(b)

Fig. 6.　Processings of the occluded region: (a) interpolation of the occluded region and (b) merging of the occluded region.
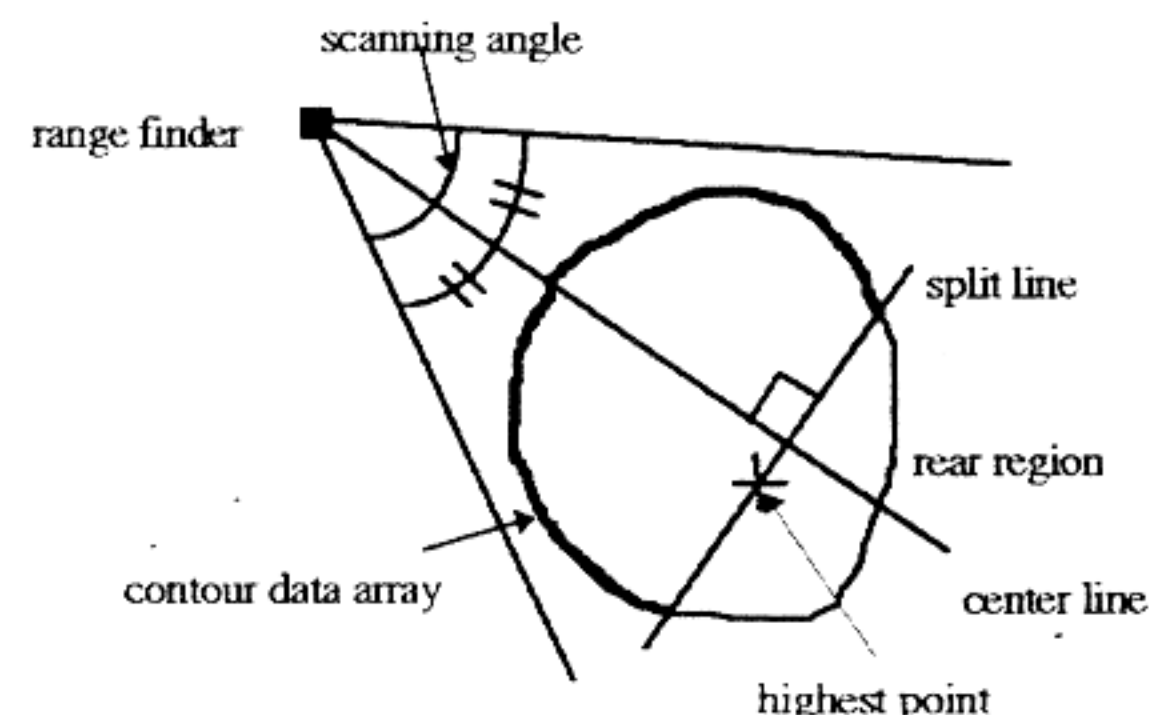
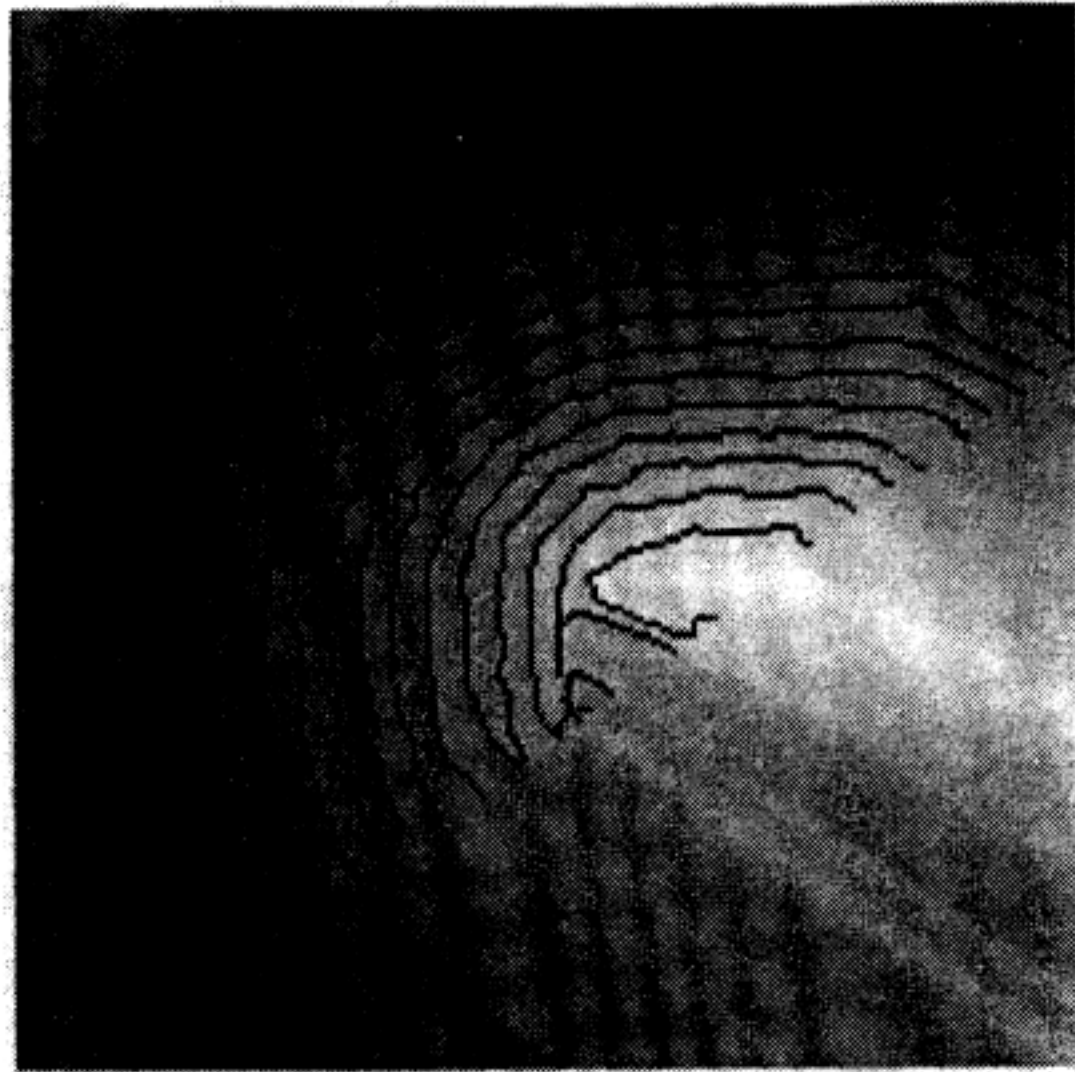

Fig. 7.　Slice for the contour line.

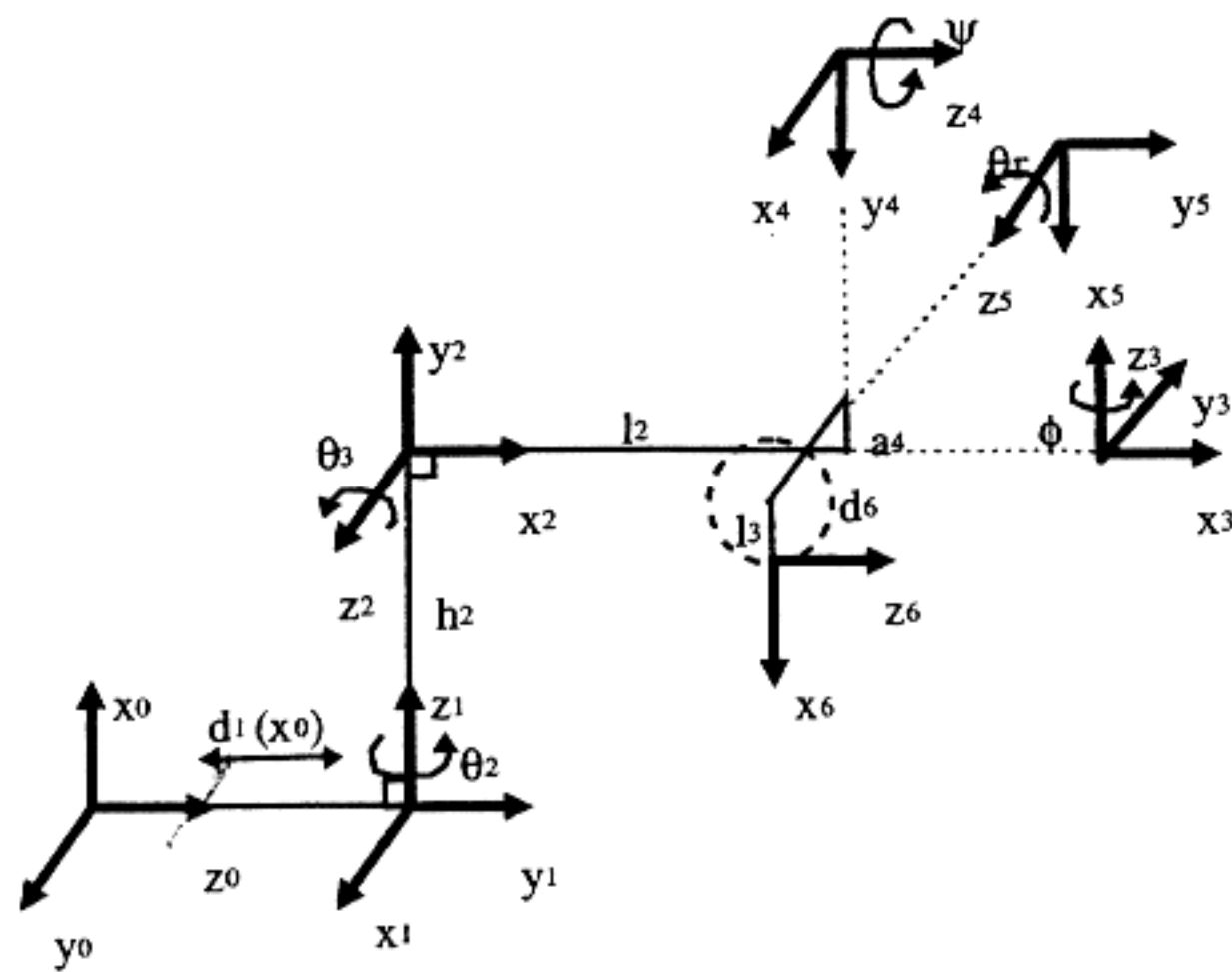Fig. 8.   Contour map for slewing operation.

Fig. 9.   Link assignment of the reclaimer.

varies according to the shape of the pile, because the bucket should contact the pile at the one point. Therefore, θ_r is another variable to be solved to determine d_1, θ_2, and θ_3.

With the link assignment, the kinematic equations are obtained as follows:

$$
\begin{aligned}
x_d = {} & \sin\theta_3(l_3\cos\phi\sin\theta_r + \sin\phi(d_6\cos\psi\cos\theta_r)) \\
& + \cos\theta_3(-l_3\cos\psi\cos\theta_r - d_6\sin\psi + a_4) \\
& + l_2\sin\theta_3 + h_2
\end{aligned}
\tag{2}
$$

$$
\begin{aligned}
y_d = {} & -\sin\theta_2(\cos\theta_3(l_3\cos\phi\sin\theta_r \\
& + \sin\phi(d_6\cos\psi\cos\theta_r)) - \sin\theta_3(-l_3\cos\psi\cos\theta_r \\
& - d_6\sin\psi + a_4) + l_2\cos\theta_3) \\
& + \cos\theta_2(\cos\phi(d_6\cos\psi - l_3\sin\psi\cos\theta_r) \\
& - l_3\sin\phi\sin\theta_r)
\end{aligned}
\tag{3}
$$

$$
\begin{aligned}
z_d = {} & \cos\theta_2(\cos\theta_3(l_3\cos\phi\sin\theta_r + \sin\phi(d_6\cos\psi \\
& - l_3\sin\psi\cos\theta_r)) - \sin\theta_3(-l_3\cos\psi\cos\theta_r \\
& - d_6\sin\psi + a_4) + l_2\cos\theta_3) \\
& + \sin\theta_2(\cos\phi(d_6\cos\psi - l_3\sin\psi\cos\theta_r) \\
& - l_3\sin\phi\sin\theta_r) + d_1.
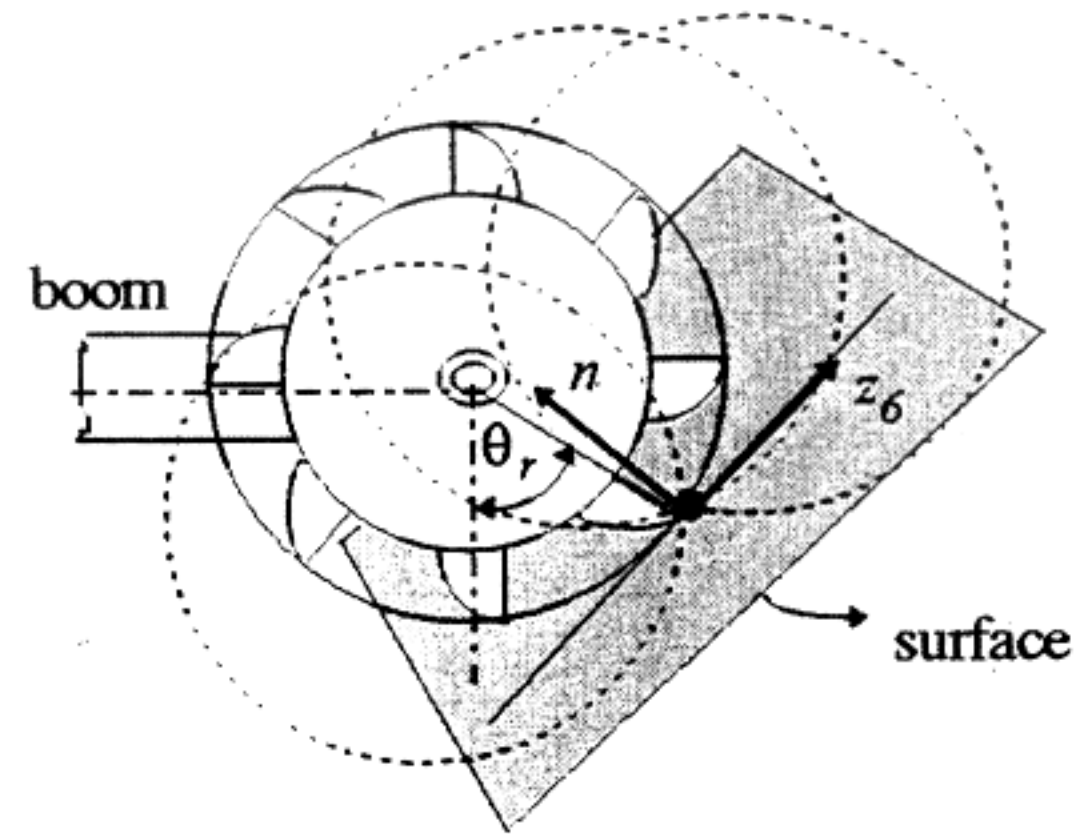\end{aligned}
\tag{4}
$$

Fig. 10.   Bucket on the estimated plane.

θ_r gives redundancy in the kinematics of the reclaimer as indicated in the above equation. Therefore, the number of the equation is fewer than that of the variables to be determined. The circles in Fig. 10 are made to be the trajectories of the rotating buckets, which means that the way that the buckets can contact with the landing point exist infinitely. But the dotted circles shows cases where the buckets are deeply embedded in the pile and they already collided with pile. Only the solid circle is desirable and θ_r is uniquely determined in this case. It gives us a constraint equation. It is derived from the fact that the circle should meet the surface of the pile at the one point.

In general, the piles have irregular curved surfaces and it is very hard to extract the mathematical model of the surface. So the plane equation in the 3-D space is more adequate in this application, because it is easily obtained using a projection method from the range data of the pile. Expressing a plane equation in the Cartesian coordinate

$$
n_x x + n_y y + n_z z = 1
\tag{5}
$$

where $n = [n_x\ n_y\ n_z]'$ is the normal vector of the plane. The reclaiming point and adjacent points $(\hat{x}_i, \hat{y}_i, \hat{z}_i)$ existing in the curved surface are selected to estimate the parameters of the plane equation. The points are determined as shown in Fig. 11. A landing point at the center of the curved plane and eight adjacent points are chosen in this scheme.

Applying the points to the plane equation

$$
\begin{bmatrix}
x_d & y_d & z_d \\
\hat{x}_1 & \hat{y}_1 & \hat{z}_1 \\
\vdots & \vdots & \vdots \\
\hat{x}_8 & \hat{y}_8 & \hat{z}_8
\end{bmatrix}
\begin{bmatrix}
n_x \\ n_y \\ n_z
\end{bmatrix}
=
\begin{bmatrix}
1 \\ 1 \\ \vdots \\ 1
\end{bmatrix}.
\tag{6}
$$

Rewriting the above equation in a simpler form

$$
W \cdot n = u
\tag{7}
$$

where $u = [1\ 1\cdots 1]'$. Since the points in the matrix W are different in the curved plane, W^{-1} is not singular. The normal vector of the plane is given as a solution of the normal equation [8] which is

$$
n = (W^T W)^{-1} W^T u.
\tag{8}
$$

From the assignment of the link frames, $z_6 = [z_{6x}\ z_{6y}\ z_{6z}]'$ is obtained as follows:

$$
\begin{aligned}
z_{6x} = {} & \cos\theta_2(\cos\phi\sin\theta_r - \sin\phi\cos\theta_r) \\
& - \sin\theta_2(\cos\theta_3\sin\phi\sin\psi\sin\theta_r + \cos\phi\cos\theta_r) \\
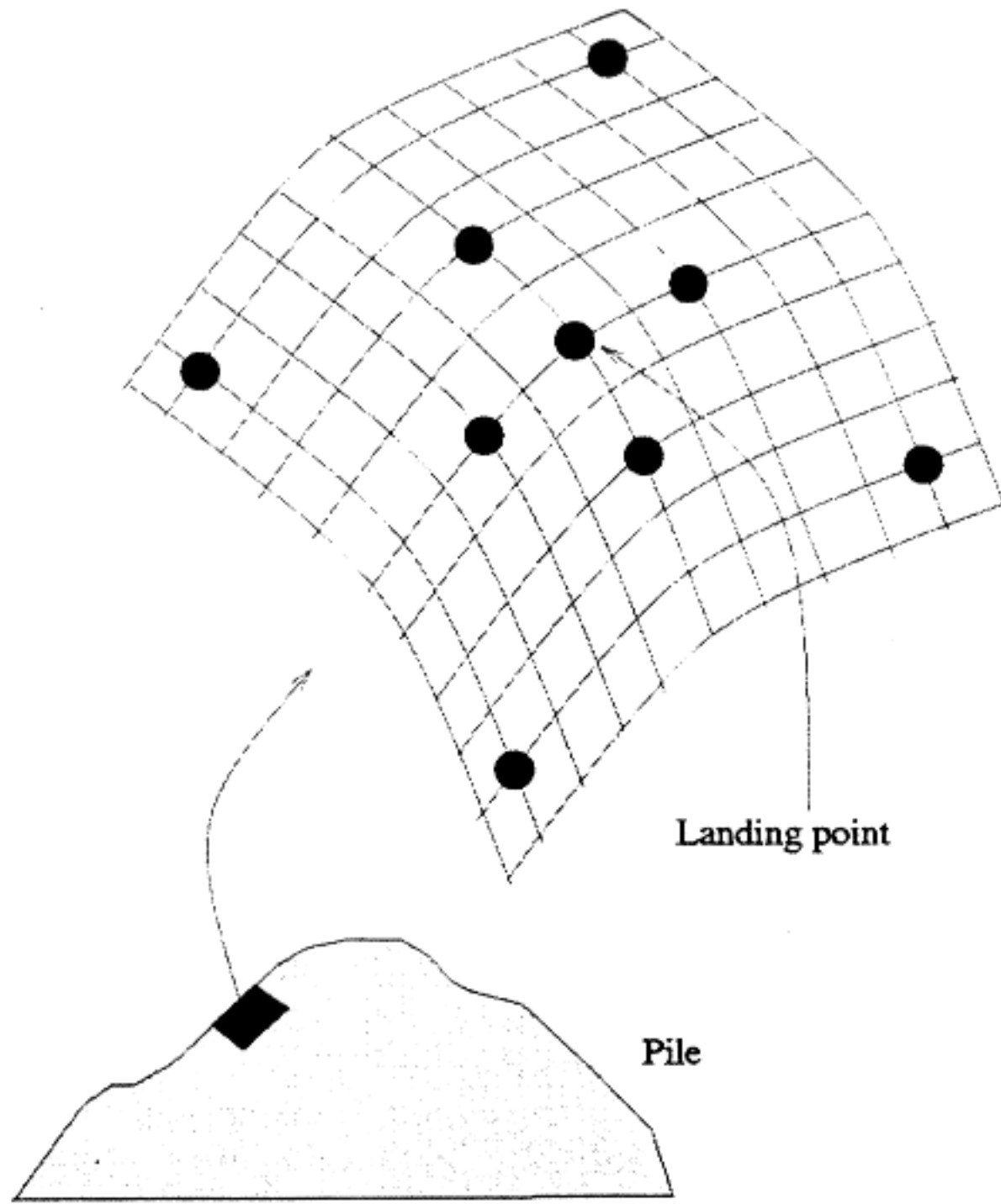& - \cos\psi\sin\theta_3\sin\theta_r)
\end{aligned}
\tag{9}
$$

Fig. 11. Selected points in the surface.

$$z_{6y} = \cos\theta_2(\cos\theta_3(\sin\phi\sin\psi\sin\theta_r + \cos\phi\cos\theta_r)$$
$$- \cos\psi\sin\theta_3\sin\theta_r) + \sin\theta_2(\cos\phi\sin\psi\sin\theta_r$$
$$- \cos\phi\cos\theta_r) \tag{10}$$
$$z_{6z} = \sin\theta_3(\sin\phi\sin\psi\sin\theta_r + \cos\phi\cos\theta_r)$$
$$+ \cos\psi\cos\theta_3\sin\theta_r. \tag{11}$$

In order that the circle of the rotating buckets meets the surface of the pile at one point, the vector z_6 and n should make a right angle. Namely, The inner product of two vectors should be 0.

Obtaining the inner product

$$f = z_6^T n = z_{6x}n_x + z_{6y}n_y + z_{6z}n_z$$
$$= n_y(\cos\theta_2(\cos\phi\sin\theta_r - \sin\phi\cos\theta_r)$$
$$- \sin\theta_2(\cos\theta_3 \cdot (\sin\phi\sin\psi\sin\theta_r + \cos\phi\cos\theta_r)$$
$$- \cos\psi\sin\theta_3\sin\theta_r)) + n_z(\cos\theta_2(\cos\theta_3$$
$$\cdot (\sin\phi\sin\psi\sin\theta_r + \cos\phi\cos\theta_r)$$
$$- \cos\psi\sin\theta_3\sin\theta_r) + \sin\theta_2(\cos\phi\sin\psi\sin\theta_r$$
$$- \cos\phi\cos\theta_r)) + n_x(\sin\theta_3(\sin\phi\sin\psi\sin\theta_r$$
$$+ \cos\phi\cos\theta_r) + \cos\psi\cos\theta_3\sin\theta_r) = 0. \tag{12}$$

The inverse kinematics problem can be solved with the forward kinematic equations and the constraint equation (12). Since the equation is highly coupled and nonlinear, analytical solutions are hard to obtain and the numerical method is used. Arranging (2) and (3)

$$x_d = \Delta_1\sin\theta_3 + \Delta_2\cos\theta_3 + h_2 \tag{13}$$
$$y_d = -\Delta_1\sin\theta_2\cos\theta_3 + \Delta_2\sin\theta_2\sin\theta_3 + \Delta_3\cos\theta_2 \tag{14}$$

where

$$\Delta_1 = l_3\cos\phi\sin\theta_r + \sin\phi(d_6\cos\psi - l_3\sin\psi\cos\theta_r) + l_2$$
$$\Delta_2 = -l_3\cos\psi\cos\theta_r - d_6\sin\psi + a_4$$
$$\Delta_3 = \cos\phi(d_6\cos\psi - l_3\sin\psi\cos\theta_r) - l_3\sin\phi\sin\theta_r.$$

Since $\Delta_1, \Delta_2, \Delta_3$ are completely determined by θ_r, (11) is the equation of θ_r and θ_3. Rewriting the equation

$$x_d - h_2 = \Delta_1\sin\theta_3 + \Delta_2\cos\theta_3$$
$$= \sqrt{\Delta_1^2 + \Delta_2^2}\,\cos(\theta_3 - \beta) \tag{15}$$

where $\cos\beta = (\Delta_1/\sqrt{\Delta_1^2 + \Delta_2^2})$ and $\sin\beta = (\Delta_2/\sqrt{\Delta_1^2 + \Delta_2^2})$. Then, β is written as:

$$\beta = \pm\arctan(\Delta_2/\Delta_1). \tag{16}$$

Dividing the both sides of (12) by $\sqrt{\Delta_1^2 + \Delta_2^2}$ and arranging it with trigonometrical relation

$$\cos(\theta_3 - \beta) = \frac{x_d - h_2}{\sqrt{\Delta_1^2 + \Delta_2^2}} \tag{17}$$

$$\sin(\theta_3 - \beta) = \sqrt{\frac{\Delta_1^2 + \Delta_2^2 - (x_d - h_2)^2}{\Delta_1^2 + \Delta_2^2}}. \tag{18}$$

Using (17) and (18), θ_3 is written as follows:

$$\theta_3 = \arctan(\Delta_2/\Delta_1)$$
$$\pm\arctan\left(\frac{\sqrt{\Delta_1^2 + \Delta_2^2 - (x_d - h_2)^2}}{x_d - h_2}\right). \tag{19}$$

θ_3 is determined with θ_r as indicated in (19). With the similar method, θ_2 is written as

$$\theta_2 = \pm\arctan\left(\frac{-\Delta_1\cos\theta_3 + \Delta_2\sin\theta_3}{\Delta_1}\right)$$
$$\pm\arctan\left(\frac{\sqrt{(-\Delta_1\cos\theta_3 + \Delta_2\sin\theta_3)^2 + \Delta_3^2 - y_d^2}}{y_d}\right). \tag{20}$$

θ_2 is also obtained with θ_3 and θ_r. The constraint equation (12) is also rewritten as the function of θ_r by applying (19) and (20). The signs in the (19) and (20) are determined by kinematic configurations of the reclaimer. The false position method [9] which is a kind of numerical method is used to obtain the joint angles. The initial value of θ_r is set between 0 and 90° by considering the stock angle of the pile. With θ_2, θ_3 and θ_r, d_1 is obtained in the (4).

IV. EXTRACTION OF A LANDING POINT

The most convex part of the pile, bulging toward the operator, is generally chosen as a landing point when well-experienced operators start to reclaim ore in the manual operation. The current procedure of the manual reclaiming operation is as follows: first, the reclaimer approaches the pile so that the buckets can gently contact with the most convex point, then the buckets are rotated to prevent abrupt collision in front of the point and lastly, the slewing operation begins while the other joints are fixed. To automate the reclaimer, an automatic landing method which is capable of substituting for the landing skill of the well-experienced operator is needed. A landing point for the buckets should be determined so as not to allow overload problems when the slewing operation is done. Let d_b be the desired digging depth of the bucket into the pile. d_b is determined according to the specific gravities of the ore and reclaiming mass per hour, etc. It is assumed that overload happens in the buckets if the buckets dig ore more deeply in the pile than the prescribed depth of the bucket.

Fig. 12 shows the contour line of the pile and the slew arc which is the trajectory of the bucket in the slewing operation. The line consists of digitized points $p_i(i = 1, \cdots, n)$. All points are assumed as possible landing points and its feasibility is investigated. If a point brings about overload in the slewing operation, it is excluded from the
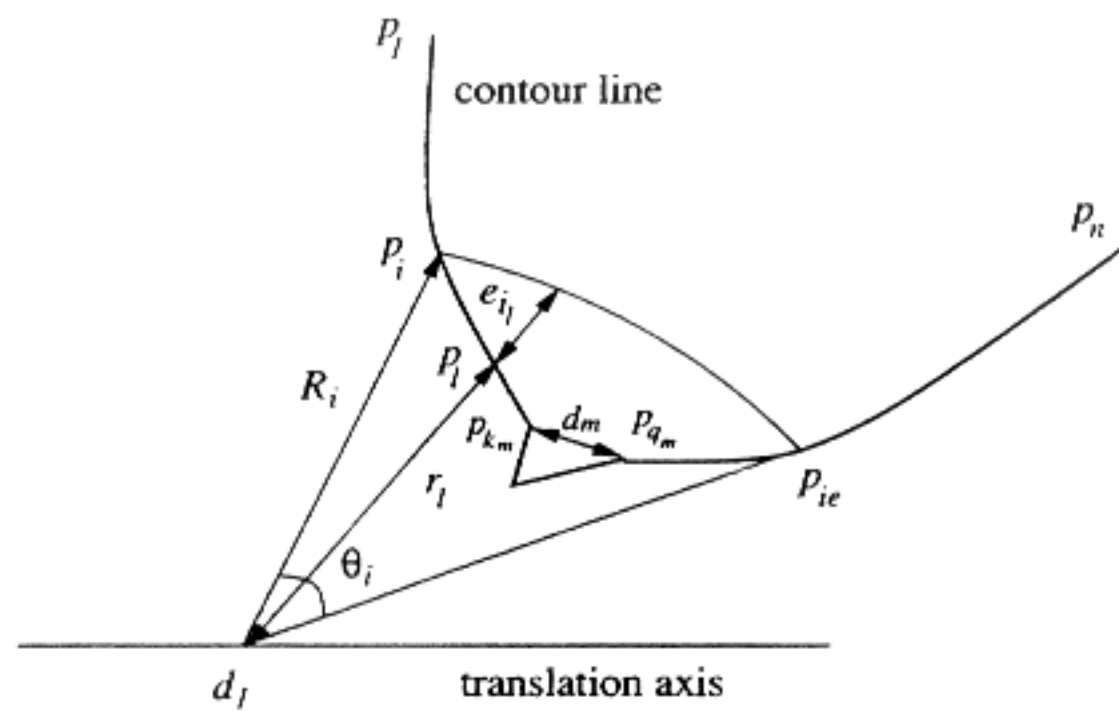
Fig. 12. Top view of the contour line and slew arc.

set of candidates of the landing points. All points on the contour line are examined if they can belong to candidates for landing points by investigating the digging depth of the bucket when it passes through the pile in the slew operation. S is defined as a set of landing point candidates. As shown in Fig. 12, the digitized contour line, in general, can have some juts, because the real contour lines of the pile have juts and the detected 3-D data have measurement noise as well. The workers usually neglect the juts if they are relatively small compared to the width and depth of the bucket to increase the reclaiming efficiency, because the allowable juts do not bring about any overload problem in the slewing operation. In this algorithm, the existences and the widths of the allowable juts are examined and they are disregarded if the width of the jut is smaller than the allowable width which is predetermined according to operation guidelines. The embedded depths of the buckets in the pile when the slewing operation is done are obtained to check the juts and determine feasible landing points. A landing point which has the maximum slew angle in the set S without causing overload is the optimal landing point, because smaller slew angle causes frequent time consuming changes of slew direction and reduced productivity.

The algorithm for extracting the optimal landing point is summarized as follows.

1) Define d_a as the allowable width of the jut.
2) FOR $i = 1$ TO n

    a)   Determine $d_1, \theta_2, \theta_3, \theta_r$ for the point p_i using the inverse kinematics.

    b)   The translation position d_1 is set to the slewing center for reclaiming.

    c)   An arc whose center is d_1 is drawn from p_i to p_{ie} where p_i and p_{ie} are the start and the end point of slewing.

    d)   Let R_i define the radius of the arc which is the trajectory of the rotating buckets in the slewing operation.

    e)   Define S_{i_l} as a set of all the points $p_l (l = 1, \cdots, j)$ on the contour curve between p_i and p_{ie}

    f)   FOR $l = 1$ TO j

        • Calculate the distance r_l from d_1 to p_l.
        • Calculate the absolute difference $e_{i_l} = |R_i - r_l|$ of R_i and r_l where e_{i_l} means the embedded depth of the buckets in the slewing operation.

    g)   ENDFOR l

    h)   Find some juts which consist of a series of points on the contour curve satisfying the condition $e_{i_l} > d_b$. That condition is also used to determine whether the buckets are deeply embedded in the pile. The mth jut consists of a series of points, $p_{k_m}, p_{k_m+1}, \cdots, p_{k_m+q_m}$ on the

contour curve between p_i and p_{ie}. $m (= 1, 2, \cdots, m_n)$ means the number of jut.

    i)   Define S_{a_i} as a set of points making up allowable juts.

    j)   FOR $m = 1$ TO m_n

        • Obtain the distance d_m between the start point p_{k_m} and the end point $p_{k_m+q_m}$ on the jut m.
        • If $d_m \leq d_a$, THEN
            • all the points on the mth jut, $p_{k_m}, p_{k_m+1}, \cdots, p_{k_m+q_m}$, belong to S_{a_i}

    k)   ENDFOR m

    l)   Obtain $S_{r_i} = S_{i_l} - S_{a_i}$. S_{r_i} contains only the points to be examined if they bring about the overload problem in the slewing operation. All the points of allowable juts are not taken into consideration.

    m)   Set

$$e_i = \max_{l \in S_{r_i}} \{e_{i_l}\}$$

        as the maximum embedded depth of the buckets when the slewing operation is done after taking p_i as the landing point.

    n)   IF $e_i \leq d_b$ THEN

        • p_i is chosen as a candidate point in which slewing operation can be done without overload. p_i becomes an element of the candidate set for the landing points S.
        • Obtain θ_i which is an angle between the landing point and slew limit.

    o)   ELSE

        • the point p_i is discarded. It can not be used as a candidate point for landing on the pile.

3) ENDFOR i
4) Obtain $\theta_{\max} = \max\{\theta_i | p_i \in S\}$ for the p_i.
5) The point p_i for the $\theta_{\max}$ is chosen as the optimal landing point. It has the widest slew angle, which is the same operation result as for the well-experienced worker.

The algorithm for extracting the optimal landing point is summarized as follows.

The obtained optimal landing point that satisfies Fig. 13 shows the graphical display for the pile and reclaimer. The scanned pile data from the range finder are reconstructed for the workers to be able to see the shape of the pile by the 3-D graphics. The reclaimer is drawn by animation techniques and the display of its on-line configuration is performed using the position data of the sensors in the joints. The contour line illustrates the reclaiming height of the pile and the optimal landing point and slew limit are extracted from the above algorithm.

V. CONCLUSIONS

An automatic landing method for choosing where to dig in a pile of raw ore was proposed to achieve autonomous reclaiming. The suggested automatic landing method is comprised of detecting the shape of a pile, extraction of contour lines of the pile, obtaining the joint angles of the reclaimer and determination of an optimal landing point.

A 3-D range finder was developed with laser radar concepts and is installed on the roof of an iron ore reclaimer to detect the ore pile contour. A topographic height map was obtained from the acquired range data for an ore pile and a contour map for the pile was obtained through some image processing steps that included
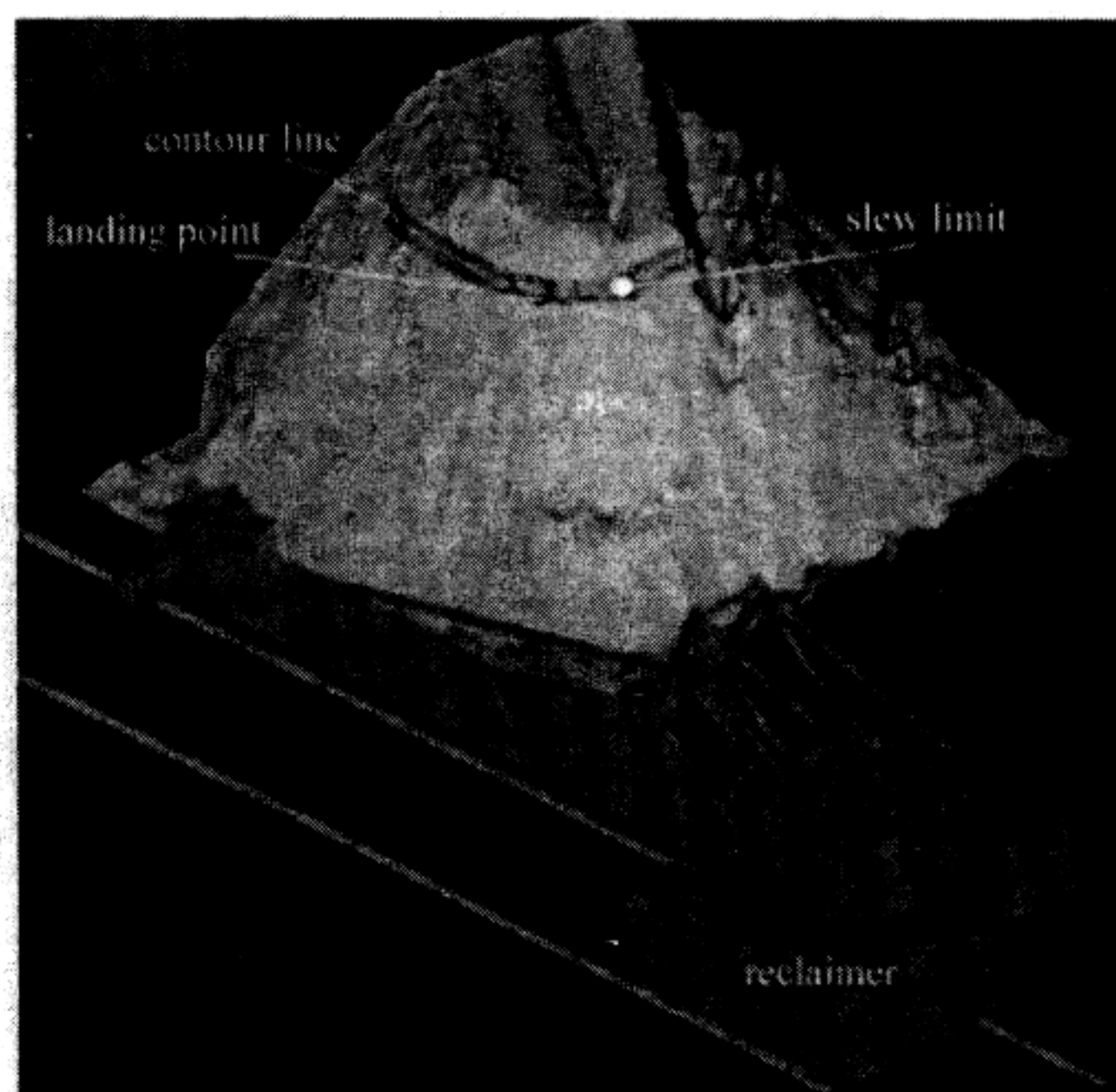
Fig. 13. Graphic display of the yard.

interpolation, merging and edge following. All the points in the contour lines were successfully examined to determine the landing point of the bucket. The optimal landing point was determined so that overload would not occur in the slewing operation and reclaiming efficiency was maximized. The algorithm for finding the landing point involved an inverse kinematics solution for the reclaimer joint angles. The reclaimer has a redundant joint due to the wheel of

rotating buckets when they land on the pile. A constraint equation based on the geometrical relationship was suggested to solve the inverse kinematics of the reclaimer with redundancy. The proposed automatic landing algorithm was successfully implemented for the reclaimer in the stockyards of Kwangyang Steelworks in Korea. Positional errors between the trajectory of the buckets and the surface of the pile are within 20 cm in the landing test. This error bound is sufficiently acceptable since the bucket length and width are about 80 and 40 cm, respectively. An autonomous reclaimer with automatic landing function is now being operated in the same site. It will be extended to all of the reclaimer in the yard and save considerable number of workers required to operate the conventional reclaimers.

REFERENCES

[1] N. Nakano and M. Katagiri, "Automatic operation method for reclaimer," *Jpn. Patents Gazette*, Patent JP56003232, 1981.
[2] T. Naka, Y. Umetsu, and K. Oshima, "Method for remote automatic operation of reclaimer," *Jpn. Patents Gazette*, Patent JP1242322, 1989.
[3] Y. Sato, T. Kawamura, and R. Yamada, "Operation method of reclaimer at the dismantled matters storage yard," *Jpn. Patents Gazette*, Patent JP58089525, 1993.
[4] V. E. Theodoracatos. and D. E. Calkins, "A 3-D vision system model for automatic object surface sensing," *Int. J. Comput. Vis.*, vol. 11, no. 1, pp. 75–99, 1993.
[5] M. Asada, M. Kimura, Y. Taniguchi, and Y. Shrai, "Dynamic integration of height maps into a 3D world representation from range image sequences," *Int. J. Comput. Vis.*, vol. 9, no. 1, pp. 31–53, 1992.
[6] D. Langer, J. K. Rosenblatt, and M. Hebert, "A behavior-based system for off-round navigation," *IEEE Trans. Robot. Automat.*, vol. 10, pp. 776–783, June 1994.
[7] R. M. Haralick and L. G. Shapiro, *Computer and Robot Vision*. Reading, MA: Addison-Wesley, 1992, vol. 1, pp. 556–558.
[8] G. Strang, *Linear Algebra and Its Applications*. Orlando, FL: Harcourt Brace Jovanovich, 1988.
[9] S. C. Chapra and R. P. Canale, *Numerical Methods for Engineers*. New York, McGraw-Hill, 1990.